EPM/RT-85-12

A CALCULATION PROCEDURE FOR THREE-DIMENSIONAL INCOMPRESSIBLE FLOWS

Marcelo Reggio and Ricardo Camarero

Ecole Polytechnique de Montréal

Avril 1985

This work was carried out with the financial support of the PRAI project #P-8122,from the NSERC of Canada and the Ministère de la Science et Technologie du Quebec.

Dépot légal , 2ème trimestre 1985
Blibliothèque nationale du Québec
Blibliothèque nationale du Canada

Pour se procurer une copie de ce document, s'adresser au:

Service de l'édition
Ecole Polytechnique de Montréal
Case Postale 6079, Succ. "A"
Montréal,Québec H3C 3A7
(514) 340-4903

Compter 0,05$ par page(arrondir au dollar le plus près),plus 1,50$(Canada) ou 2,50$(étranger) pour la couverture,les frais de poste et la manutention.Régler en dollars canadiens par chèque ou mandat-poste au nom de l'Ecole Polytechnique de Montréal.Nous n'honorerons que les commandes accompagnées d'un paiement,sauf s'il y a eu entente préalable, dans le cas d'établissements d'enseignement ou d'organismes canadiens.

ABSTRACT

A time dependent calculation procedure to solve the incompressible Navier-Stokes equations in arbitrary three-dimensional shapes is presented. The conservative form of the primitive-variable formulation written for a general curvilinear coordinate system is adopted. The numerical scheme is based on an overlapping grid with opposed differencing for mass and pressure gradients. This structure allows the use of the same computational cell for the continuity and the momentum equations,and yet no spurious oscillations in the velocity or pressure fields are present. The method is applied to test cases of ducting and the results are compared with experimental and numerical data.

1. INTRODUCTION

Progress of the design process in turbomachinery demands a maximization of the power recovery while at the same time a minimization of the machine size. This could mean, for example, that the blade loading has to be increased in order to reduce the number of blades.

The ability to respond to this kind of conflicting requirements is related to the availability of appropriate analysis tools.In this context the prediction of the three dimensional physics inside a blade passage is crucial. The main difficulties associated with the solution of this type of problem are: the treatment of the boundary conditions on the geometries that bounds the domain,the choice of a proper storage location for the dependent variables and the lack of an explicit equation for the pressure.

The objective of this report is to present a numerical procedure to solve three-dimensional time-dependent incompressible Navier-Stokes equations inside turbine blade rows. The proposed method is based on the primitive-variable formulation using a control volume approach.

The problem of the complex boundaries is treated by formulating and solving the conservation equations on a curvilinear coordinate system that matches the boundary domain. Because the boundary nodes always coincide with the domain boundary, no particular procedure is

required at these locations.

Different techniques can be used to numerically create a curvilinear mesh, a detailed review of the subject has been given in [1]; also a specific 3-D generation procedure developed by the authors can be found in [2].

Currently the computational discretization used for solving incompressible fluid flow problems is the staggered grid. This technique avoids the checkerboard pattern for velocity and pressure fields,however it requires a different location, together with a distinct computational cell for each velocity component and the pressure.In the present study it is proposed to compute the pressure and the velocity components at the same grid location. These parameters are located at the center of the same computational cell which is used for the momentum and continuity balance. As a result the computer implementation of the present method is much simpler than the staggered grid approach, because fewer geometric terms are required, and smaller memory space is needed. To avoid the checkerboard pattern for the pressure or velocity fields, that normally would appear with such discretization, an opposed difference scheme for pressure and fluxes is used in the main flow direction.

The coupling between the pressure and velocity fields is obtained by means of a pressure equation based on the SIMPLE method[3]. This procedure was derived for a curvilinear grid and applied to attain a pressure field which drives velocities that

satisfy the mass conservation.

The present method has been applied to obtain the numerical solution of flows within ducts of different geometries.The results reveal the complex nature of the three dimensional phenomena showing some aspects of the secondary flow. This scheme,coupled with an automatic mesh generator,is a promising tool for the blade row analysis.

2. CONSERVATION EQUATIONS

When formulating the equations of motion on a fully curvilinear system, additional source or sink terms appear in these equations.These terms represented by Christoffel symbols are due to the required connection between different points of the space that belongs to a different vector basis.Although such an approach has been previously used [4,5],it is felt that in order to avoid the numerical complications created by such terms the strong conservative formulation is preferable.This means that the cartesian momentum components are kept as the dependent variables, rather than the contravariant components. This results in an hybrid system which is not more complicated than their cartesian counterpart.

Following this approach the time dependent Navier-Stokes equations can be written as:

$$\frac{\partial q}{\partial t} + \frac{\partial E}{\partial \xi} + \frac{\partial F}{\partial \eta} + \frac{\partial G}{\partial \zeta} = \frac{\partial R}{\partial \xi} + \frac{\partial S}{\partial \eta} + \frac{\partial T}{\partial \zeta} \qquad (1)$$

where ξ represents the "streamwise" direction, η ,the "normal" direction and ζ the "binormal" direction as illustrated in Fig 1.

The flux and diffusion terms in Eq.(1) are:

$$q = J \begin{bmatrix} 0 \\ u \\ v \\ w \end{bmatrix} \qquad E = J \begin{bmatrix} U \\ uU + p\xi_x \\ vU + p\xi_y \\ wU + p\xi_z \end{bmatrix} \qquad F = J \begin{bmatrix} V \\ uV + p\eta_x \\ vV + p\eta_y \\ wV + p\eta_z \end{bmatrix} \qquad G = J \begin{bmatrix} W \\ uW + p\zeta_x \\ vW + p\zeta_y \\ wW + p\zeta_z \end{bmatrix}$$

$$R = \mu J \begin{bmatrix} 0 & & \\ g^{11}u_\xi + g^{12}u_\eta & g^{13}u_\zeta \\ g^{11}v_\xi + g^{12}v_\eta & g^{13}v_\zeta \\ g^{11}w_\xi + g^{12}w_\eta & g^{13}w_\zeta \end{bmatrix}$$

$$S = \mu J \begin{bmatrix} 0 & & \\ g^{21}u_\xi + g^{22}u_\eta & g^{23}u_\zeta \\ g^{21}v_\xi + g^{22}v_\eta & g^{23}v_\zeta \\ g^{21}w_\xi + g^{22}w_\eta & g^{23}w_\zeta \end{bmatrix}$$

$$T = \mu J \begin{bmatrix} 0 & & \\ g^{31}u_\xi + g^{32}u_\eta & g^{33}u_\zeta \\ g^{31}v_\xi + g^{32}v_\eta & g^{33}v_\zeta \\ g^{31}w_\xi + g^{32}w_\eta & g^{33}w_\zeta \end{bmatrix}$$

where μ represents the viscosity.

The cartesian velocity components u,v,w and the contravariant velocity components U,V,W along the curvilinear coordinates ξ,η and ζ are related by:

$$\begin{aligned} U &= u\xi_x + v\xi_y + w\xi_z \\ V &= u\eta_x + v\eta_y + w\eta_z \\ W &= u\zeta_x + v\zeta_y + w\zeta_z \end{aligned} \qquad (2)$$

The metric terms ξ_x, ξ_y, ξ_z, etc , the jacobian J and the contravariant metric tensor components g_{ij}, are obtained from:

$$\xi_x = (y_\eta z_\zeta - y_\zeta z_\eta)/J \qquad \eta_x = (z_\zeta z_\xi - y_\zeta z_\xi)/J$$

$$\xi_y = (z_\eta x_\zeta - x_\eta z_\zeta)/J \qquad \eta_y = (x_\zeta z_\xi - x_\xi z_\zeta)/J$$

$$\xi_z = (x_\eta y_\zeta - y_\eta x_\zeta)/J \qquad \eta_z = (y_\zeta x_\xi - x_\zeta y_\xi)/J$$

$$\zeta_x = (y_\zeta z_\eta - z_\zeta y_\eta)/J$$

$$\zeta_y = (x_\eta z_\zeta - x_\zeta z_\eta)/J$$

$$\zeta_z = (x_\zeta y_\eta - y_\zeta x_\eta)/J$$

$$J=x_\xi y_\eta z_\zeta+x_\zeta y_\xi z_\eta+x_\eta y_\zeta z_\xi-x_\xi y_\zeta z_\eta-x_\eta y_\xi z_\zeta-x_\zeta y_\eta z_\xi$$

$$g_{ij} = \frac{\partial}{\partial \xi^i}\frac{x_k}{\xi^i}\frac{\partial x_k}{\partial \xi^j}$$

with $\xi^1 = \xi$, $\xi^2 = \eta$, $\xi^3 = \zeta$

3. DISCRETIZATION

As mentioned earlier a grid structure frequently utilized to approximate the spatial derivatives of the Navier-Stokes equations is the staggered grid formulation introduced by Harlow and Welch[6].In this approach the pressure is stored at the center of the cell while the velocity components are defined at the cell faces.This disposition avoids a zigzag pattern for the velocity and pressure fields,but demands a different location for the pressure and for every velocity component .Although its implementation using the conservative form is possible (see for example Ref[7]) it requires the storage of more than one velocity component at each face and the computer implementation becomes difficult.

In the present work a different scheme and corresponding grid arrrangement is proposed.The discretization is based on an overlapping grid structure where the basic cell is made of one unit in the main flow direction and two units in the two directions. Fig 2. shows a two dimensional cell structure on the computational ξ-η (k=const.)plane

for ease of visualisation. Fig.3. depicts the general cell in three-dimensions. In the present formulation the pressure and cartesian velocity components are stored at the center of such cells.

In applying the basic equations to this grid structure, central differences are used to evaluate mass and pressure gradients in the η and ζ directions.This yields a system of equation which require the values of velocity at the j+1,k and j-1,k and j,k-1 and j,k+1 faces. These are not interpolated but are calculated by overlapping elements in those directions. The pressure is obtained by the averaging of two neighbouring points in each direction.

To gain insight of this overlapping procedure, an explanation in 2-D is attempted for a k=const. plane with this latter subscript omitted.

When solving the system (1) cartesian and curvilinear components are required. The first set of components are calculated and stored at the center i+1/2,j of the element(Fig 2.). As a result of the overlapping procedure in the j direction that is illustrated on Fig.4, these properties are also known at the i+1/2,j+1 location that correspond to the center of the cell half unit above. The same reasoning applies for the j-1 ,k+1, and k-1 levels.

With the known cartesian velocity components at all j and k levels the V and W components are computed from Eq.(2) as:

$$V_{i+1/2,j\pm1} = u_{i+1/2,j\pm1}(\eta_x)_{i+1/2,j\pm1} + v_{i+1/2,j\pm1}(\eta_y)_{i+1/2,j\pm1} + w_{i+1/2,j\pm1}(\eta_z)_{i+1/2,j\pm1}$$

for k=const.

and

$$W_{i+1/2,k\pm1} = u_{i+1/2,k\pm1}(\zeta_x)_{i+1/2,k\pm1} + v_{i+1/2,k\pm1}(\zeta_y)_{i+1/2,k\pm1} + w_{i+1/2,k\pm1}(\zeta_z)_{i+1/2,k\pm1}$$

for j=const.

In the "streamwise" direction ξ no averaging or overlapping is used. The treatment is done by combining forward and backward differences. Mass gradients are obtained by upwind differencing,so the flux through the downstream i+1,j,k face is controlled by the velocity located at the center of the cell i+1/2,j,k.With this in mind the U components are obtained for the k=const. levels as:

$$U_{i,j} = u_{i-1/2,j}(\xi_x)_{i,j} + v_{i-1/2,j}(\xi_y)_{i,j} + w_{i-1/2,j}(\xi_z)_{i,j}$$

Pressure gradients are calculated by downwind differencing ,this can be interpreted as if the pressure at the center of the element

acts on its the upstream face i,j,k.

The following u momentum equation summarizes the employed discretization.

$$J_{i+1/2,j,k}\frac{(u^{n+1}-u^{n})_{i+1/2,j,k}}{\Delta t}$$

$$+\ \frac{(JuU)_{i+1,j,k}-(JuU)_{i,j,k}}{\Delta\xi}$$

$$+\ \frac{(JuV)_{i+1/2,j+1,k}-(JuV)_{i+1/2,j-1,k}}{2\Delta\eta}$$

$$+\ \frac{(JuW)_{i+1/2,j,k+1}-(JuW)_{i+1/2,j,k-1}}{2\Delta\eta}$$

$$+\ \frac{p_{i+3/2,j,k}(J\xi_x)_{i+1,j,k}-p_{i+1/2,j,k}(J\xi_x)_{i,j,k}}{\Delta\xi}$$

$$+\ \frac{p_{i+1/2,j+1,k}(J\eta_x)_{i+1/2,j+1,k}-p_{i+1/2,j-1,k}(J\eta_x)_{i+1/2,j-1,k}}{2\Delta\eta}$$

$$+\ \frac{p_{i+1/2,j,k+1}(J\zeta_x)_{i+1/2,j,k+1}-p_{i+1/2,j,k-1}(J\zeta_x)_{i+1/2,j,k-1}}{2\Delta\zeta}$$

$$+\ VIS\ =\ 0$$

where VIS represents the resulting viscous terms over the element.

An analogous scheme has been used by Denton[8] for the solution of the compressible Euler equations.A comparable scheme together with an interesting explanation of the opposed-differencing idea can be found in Ref[9].Recently Fuchs[10] has also used a combination of backward and forward differences coupled with the multigrid technique.These last two references solve the steady state equations.

To evaluate the convected momentum term at the cell faces, the

weighted upstream difference scheme of Raithby and Torrance[11] has been adopted.These authors propose the use of weights depending on the Peclet number to calculate the degree of upwinding.

4. BOUNDARY CONDITIONS

4a) Velocity

As in the present approach both cartesian and curvilinear velocities take part in the calculation procedure, boundary conditions should be given for both of them.

At the inlet a velocity profile in terms of the cartesian and contravariant components is specified.

At a no-slip surface only one curvilinear component has to be supplied, because the remining two do not contribute to the flow balance over the adjacent elements to these surfaces. This means for example that for the triad U,V,W along the ξ,η,ζ coordinates,only the W component is needed at a wall coincident with a ξ-η surface; and this value is zero.

In spite of that the null mass flow is assured at the solid walls by the boundary condition on the curvilinear components, the cartesian velocity components are also required ;they simply are u=v=w=0.

At the outflow boundary zero gradient of the curvilinear

weighted upstream difference scheme of Raithby and Torrance[11] has been adopted.These authors propose the use of weights depending on the Peclet number to calculate the degree of upwinding.

4. BOUNDARY CONDITIONS

4a) Velocity

As in the present approach both cartesian and curvilinear velocities take part in the calculation procedure, boundary conditions should be given for both of them.

At the inlet a velocity profile in terms of the cartesian and contravariant components is specified.

At a no-slip surface only one curvilinear component has to be supplied, because the remining two do not contribute to the flow balance over the adjacent elements to these surfaces. This means for example that for the triad U,V,W along the ξ,η,ζ coordinates,only the W component is needed at a wall coincident with a ξ-η surface; and this value is zero.

In spite of that the null mass flow is assured at the solid walls by the boundary condition on the curvilinear components, the cartesian velocity components are also required ;they simply are u=v=w=0.

At the outflow boundary zero gradient of the curvilinear

components is specified from which the cartesian components are derived.

4b) Pressure

No physical boundary condition is specified for the pressure at any boundary location. However this parameter is needed at such stations, and a numerical boundary condition has to be applied.

The values at the solid walls are obtained via a parabolic extrapolation from the interior points. This guarantees a second order approximation consistent over the entire computational domain.

At the inflow boundary no condition is needed for the pressure because the downwind scheme.

At the outflow boundary a simple linear extrapolation is used, because the numerical error introduced by this calculation is not expected to propagate upstream.

5. SOLUTION PROCEDURE

The scheme is explicit and in a general form can be written as:

$$\Delta q + \Delta t (E_\xi + F_\eta + G_\zeta)^n = \Delta t (R_\xi + S_\eta + T_\zeta)^n \qquad (3)$$

components is specified from which the cartesian components are derived.

4b) Pressure

No physical boundary condition is specified for the pressure at any boundary location. However this parameter is needed at such stations, and a numerical boundary condition has to be applied.

The values at the solid walls are obtained via a parabolic extrapolation from the interior points. This guarantees a second order approximation consistent over the entire computational domain.

At the inflow boundary no condition is needed for the pressure because the downwind scheme.

At the outflow boundary a simple linear extrapolation is used, because the numerical error introduced by this calculation is not expected to propagate upstream.

5. SOLUTION PROCEDURE

The scheme is explicit and in a general form can be written as:

$$\Delta q + \Delta t (E_\xi + F_\eta + G_\varsigma)^n = \Delta t (R_\xi + S_\eta + T_\varsigma)^n \qquad (3)$$

where Δ denotes the forward time difference operator and the superscript n the time level.

The sequence of calculations is as follows.A velocity and pressure field are first guessed. Then the three cartesian momentum components characterized by Eq. (3) are solved to get three velocity components over the whole domain. These intermediate values do not satisfy mass conservation.

The next step is to adjust the pressure field in order to satisfy the continuity equation. To handle the velocity-pressure coupling the principle of the SIMPLE method[3] is followed.By using the momentum equations, the corrections to the contravariant velocity components are related to the corrections to the pressure as follows:

$$\begin{aligned} \delta U &= f^{U}(\delta p) \\ \delta V &= f^{V}(\delta p) \\ \delta W &= f^{W}(\delta p) \end{aligned} \qquad (4)$$

Introducing these expressions into the continuity equation a pressure adjustment is derived:

$$\delta p = f^{P}(\delta U, \delta V, \delta W) \qquad (5)$$

Once the pressure correction δp is calculated,the curvilinear velocity components are modified by means of Eq.(4),then all corrections are combined with the inexact velocity and pressure fields in order to verify the mass constraint requirement. That is,

$$\begin{aligned} U &= U^* + \delta U \\ V &= V^* + \delta V \\ W &= W^* + \delta W \\ p &= p^* + \delta p \end{aligned} \qquad (6)$$

where U,V,W,p and U^*,V^*,W^*,p^* represent those values that do and do not respectively satisfy both mass and momentum equations.

To modify these variables over the entire domain a similar practice to the MAC method[12] is used.The grid is swept point-by-point in sucessive planes in the inlet-outlet direction.Improved values are immediately used as the procedure advances.This is repeated until a desired level of accuracy is reached.

When the above step is completed,only one curvilinear velocity component is known on each face(U,V,W on the $\xi,\eta,$and ζ faces respectively).The two missing missing contravariant components are obtained by averaging surrounding known values. The cartesian velocity components are decoded by using the inverse

relations of Eqs.(2).

Finally the time step is advanced and the cycle is repeated until steady state is reached. This is estimated by comparing the root mean square of a velocity component between two consecutives time steps.

6. APPLICATIONS

At the present stage and as a preliminary step, a series of test cases on ductings have been done.

6.1 Exponential Constriction

In order to analyze the response of the method on a curvilinear geometry the "hump test case" fully tested by Refs [13,14], who used a vector potential difference method was chosen.This geometry consists of channel with an exponential constriction where the function $y=1.-.5e^{-2x}$ represents the lower surface for all depths;while y=1. represent the flat upper surface.The mesh used was of 31x11x11 points.

Figure 5a shows a general view of the duct shape , Fig 5b gives the geometric characteristics for all ζ=const. planes.

A developed profile specified as $u=36yz(1-y)(1-z)$, $v=0.$,

relations of Eqs.(2).

Finally the time step is advanced and the cycle is repeated until steady state is reached. This is estimated by comparing the root mean square of a velocity component between two consecutives time steps.

6. APPLICATIONS

At the present stage and as a preliminary step, a series of test cases on ductings have been done.

6.1 Exponential Constriction

In order to analyze the response of the method on a curvilinear geometry the "hump test case" fully tested by Refs [13,14], who used a vector potential difference method was chosen.This geometry consists of channel with an exponential constriction where the function $y=1.-.5e^{-2x}$ represents the lower surface for all depths;while y=1. represent the flat upper surface.The mesh used was of 31x11x11 points.

Figure 5a shows a general view of the duct shape , Fig 5b gives the geometric characteristics for all ζ=const. planes.

A developed profile specified as u=36yz(1-y)(1-z), v=0. ,

w=0. is set at the inlet and several tests were conducted for different Reynolds numbers.

The results shown on Fig. 6a report a view of the isopressure contours on the outmost surfaces obtained for a Reynolds number of 80.

Figure 6b shows the velocity field in the obstruction planes z=0.1 and z=0.5. The recirculation zone downstream of the obstruction and the shape of the velocity profile at the exit plane confirm the results obtained by Lacroix et al [13].

The flow pattern viewed from the top is shown in Fig. 6c. The developing velocity profile at the outlet indicate that the channel is not sufficiently long for the flow to re-establish itself after the constriction.The shape of the velocity profile at outlet at the η=0.9 and η=0.5 surfaces harmonize with those reported by Ref.14, but not at the η=0.1 level where a parabolic profile is attained in the present computations, while a profile with an inflection is obtained by Ref.14.

The velocity vectors in ξ=constant sections are presented in Fig. 6d. Eventhough these section are not strictly normal to the primary flow motion, an interesting three-dimensional phenomena can still be observed. When the flow reaches the obstruction the bottom surface layer is forced towards the center line. As it falls down the rear of the constriction, this layer is forced towards the centerline.Finally two symmetric vortices are developed .

6.2 Circular Channel

A second investigation was done in a circular arc channel of square cross section with a Reynolds number of 80. For this case the Dean number defined as:

$$De=Re(H/R_m)^{0.5} \qquad (7)$$

is 50.95964 ,where H=1 is the radial distance in the channel,and R_m=2.5 is the channel mean radius of curvature. Upstream and downstream lengths of a straight channel of 0.524H and 2.1H respectively are attached to the curved duct. The turning angle of the elbow is 60 degrees .In the streamwise direction 31 stations were used , while 11x11 points were used for the cross section (Fig 7a).

As in the previous case a parabolic velocity profile with no transverse component was set at the inlet.

The distribution of the pressure on the outmost surfaces is shown on Fig. 7b by contours of constant values of the pressure. The importance of the viscous influence can be appreciated if one compares this result with the potential pressure solution obtained by Herong[14] ,Fig. 7c.

The velocity field is shown on differents ζ surfaces(planes in this case) in Fig.7d, whereas Fig. 7e depicts it in several projections of the η=constant surfaces .

The developement of secondary flow is illustated in Fig 7f. From the beginning of the turning angle this helical motion can be noticed and as the flow progresses in the channel, low momentum fluid is drawn from the side wall and convected downstream towards the suction surface and high streamwise velocities near the centerline are displaced accordingly toward the pressure surface. At the exit the secondary flow is not as strong but still does not disappear entirely because the downstream extension is not sufficiently long to allow a re-development of the flow.

To assess the present solution a comparison of the computed fully developed streamwise velocity profile with the experimental measurements obtained by Mori et al [15] at Re=205 has been carried out . This is illustrated on Fig. 7g which shows good qualitative and quantitative agreement of both results.However the present numerical data does not coincide with the results obtained by Refs(14,16,17,18)

6.3 Twisted Elbow

As the aim of the present effort is the simulation of a 3-D flow in an arbitrary channel such as the geometry bounded by the blades of a turbomachine, a final numerical application was carried out to show the fully three dimensional prediction capability

of the present model.

The channel chosen is shown in Fig. 8a and its geometric characteristics were devised by Herong[14]. As the elbow discussed before, the cross section is a square, the upstream and downstream tangents have the same lengths, the turning angle is 60 degrees and the discretization was carried using 31x11x11 mesh points.However,this time the turning elbow has a 60 degrees twist around its central line,so the three-dimensionality is fully present.

As in the previous models a parabolic profile was set at the inlet with no transverse components.

Figure 8b shows the presure plotted in contours of constant values viewed from opposite directions.

The velocity distribution is shown in Figs.8c and 8d. Each drawing presents the velocity vector in one coordinate surface family within the elbow configuration,the first in ξ=constant surfaces, while the second in η=constant surfaces.

A very interesting phenomena in such a complex geometry is the developement of the secondary flow, which is presented in Fig.8e. It consists on the generation of a vortex pair that remains normal to the plane of the duct turning. The twisting seems to have no effect on the location of the vortices;however it does increase the strength of one side of the vortex pair, while decreasing the other. This influence becomes more evident after θ=40°(Fig. 8e).

After the channel stops twisting and turning at $\theta=60°$, the flow begins to recover ,but as the length of the downstream tangent is relatively short for the present case of Re=80. still cannot reach the straight channel flow type.

7. CONCLUDING REMARKS

The preliminary goal of the present work was the development of a numerical procedure to solve 3-D incompressible flows on general geometries with a non-staggered grid formulation.This was accomplished by the use of an opposed difference scheme. A typical computation for 31 x 11 x 11 grid points,with no particular attention to speed up the convergence is about 20 minutes of C.P.U. time on a IBM 4341-II.

The reported results are encouraging ,as the proposed method predicts most of the complex nature of the three-dimensional viscous flow phenomena inside ductings with a plausible estimate of the characteristics of the secondary flow.

REFERENCES:

(1) Thompson,J.F., "Grid Generation Techniques in Computational Fluids Dynamics " AIAA Journal,Vol. 22 ,No 11 ,1984 ,pp 1505-1523

(2) Camarero,R. and Reggio,M., "A Multigrid Scheme for Three-Dimensional Body-Fitted Coordinates in Turbomachine Applications",Journal of Fluids Engineering,Vol 105,1983,pp 76-82

(3) Patankar,S.V., Numerical Heat Transfer and Fluid Flow Hemisphere Publishing Corporation,Washington,D.C.,1980

(4) Hsu.C-F., " A Curvilinear-Coordinate Method Momentum,Heat and Mass Transfer in Domains of Irregular Geometry",Ph. D. Thesis, University of Minessota,1982

(5) Nakayama, Akira., "A Finite Difference Calculation Procedure for Three-Dimensional Turbulent Separated Flow",Int. J. Numer. Methods Eng. Vol. 20 ,1984,pp 1247-1260

(6) Harlow,F.H and Welch, J.E., "Numerical Calculation of Time Dependent Viscous Incompressible Flow of Fluid with Free Surface", Physics of Fluids, Vol. 8, 1965, pp 2182-2189

(7) Maliska, C.R., "A Solution Method for Three-Dimensional Parabolic Fluid Flow Problems in Nonorthogonal Coordinates", Ph. D. Thesis, University of Waterloo,Canada,1981

(8) Denton, J.D., "A Time Marching Method for Two and Three Dimensional Blade-to-Blade Flows", A.R.C., REM 3775 ,1975

(9) Roscoe, D.F., "The Numerical Solution of the Navier-Stokes Equations for Three-Dimensional Laminar Flow in Curved Pipes using Finite Differences Methods", J. of Engineering Mathematics,Vol 12, 1978, pp 303-323

(10) Fuchs, L. and Zhao H-S., "Solution of Three-Dimensional Viscous Incompressible Flow By A Multigrid Method", Int. Journal for Numerical Methods in Fluids, Vol. 4, 1984, pp 539-555

(11) Raitby, G.D and Torrance, K.E., "Upstream Weighted Differencing Schemes and their Application to Elliptic Problems Involving Fluid Flows", Computer Fluids, Vol. 2, 1974, pp 191-206

(12) Hirt, C.W., Nichols, B.D and Romero, N.C., " SOLA- A Numerical Solution Algorithm for Transient Fluid Flows", Report LA-5852 ,1975, Los Alamos Scientific Labortory, Los Alamos,NM.

(13) Lacroix, M., Camarero, R. and Tapucu, A. "Etude d'écoulements Internes Tridimensionnels" EP84-R-9 ,1984, Ecole Polytechnique de Montréal

(14) Herong, Y., and Camarero, R. "Numerical Modeling of Threee-Dimensional Viscous Incompressible Steady-State Duct Flow Using Body-fitted Coordinate System",EPM/RT-85-3, Ecole Polytechnique

de Montréal; also International Journal for Numerical Methods in Fluids, to be published.

(15) Mori, Y., Uchida, Y., and Ukon T., "Forced Convective Heat Transfer in a Curved Channel with a Square Cross Section", Int J.Heat and Mass Transfer Vol 14, 1971 p 1781

(16) Kreskovsky, J.P., Briley, W. R., and McDonald, H., " Prediction of Laminar and Turbulent Primary and Secondary Flows in Strongly Curved Ducts, " NASA CR3388,1981.

(17) Ghia, K.N., Sokhey, J.S., " Analysis and Numerical Solution of Viscous Flows in Curved Ducts of Rectangular Cross Section," Numerical/Laboratory Computer Methods in Fluid Mechanics, ASME, New York, 1976.

(18) Khalil, I.M., Weber H.G., " Modeling of Three-Dimensional Flow in Turning Channels," ASME, Journal of Engineering for Power, Vol 106, pp. 682-691, 1984.

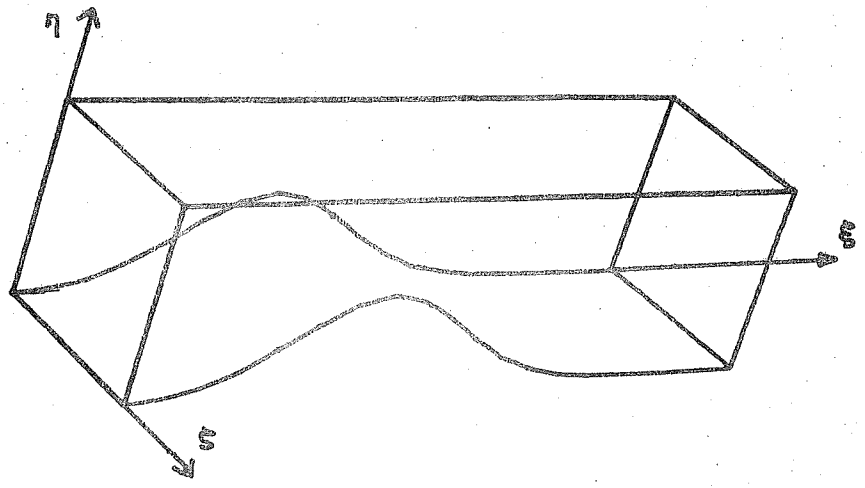

Fig.1 Curvilinear Axes (Physical Domain)

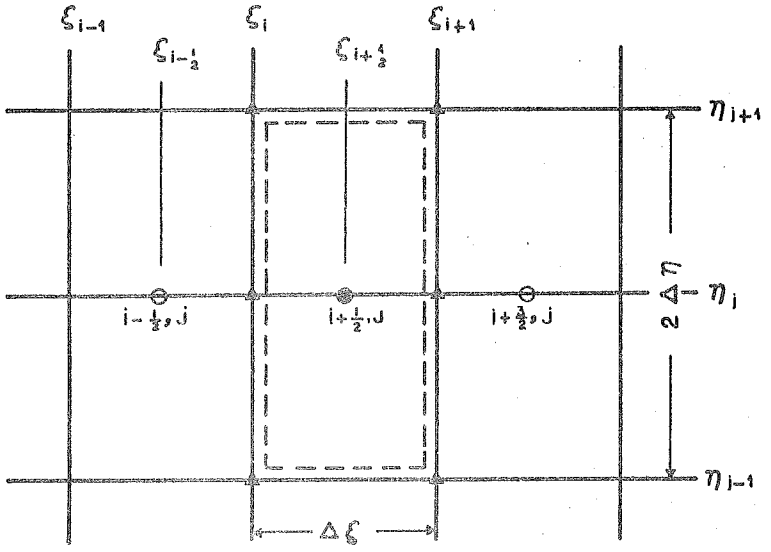

Fig.2 Computational Cell in a plane ζ=const.

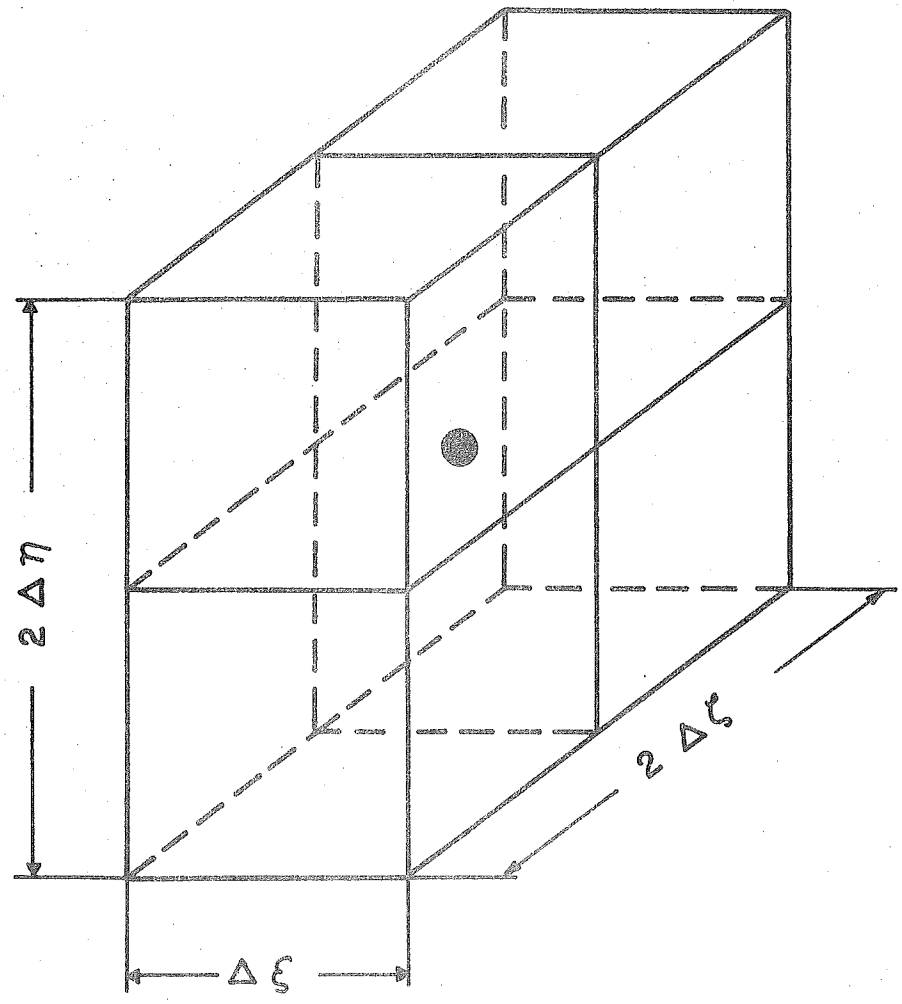

Fig.3 Computational Three-Dimensional Cell

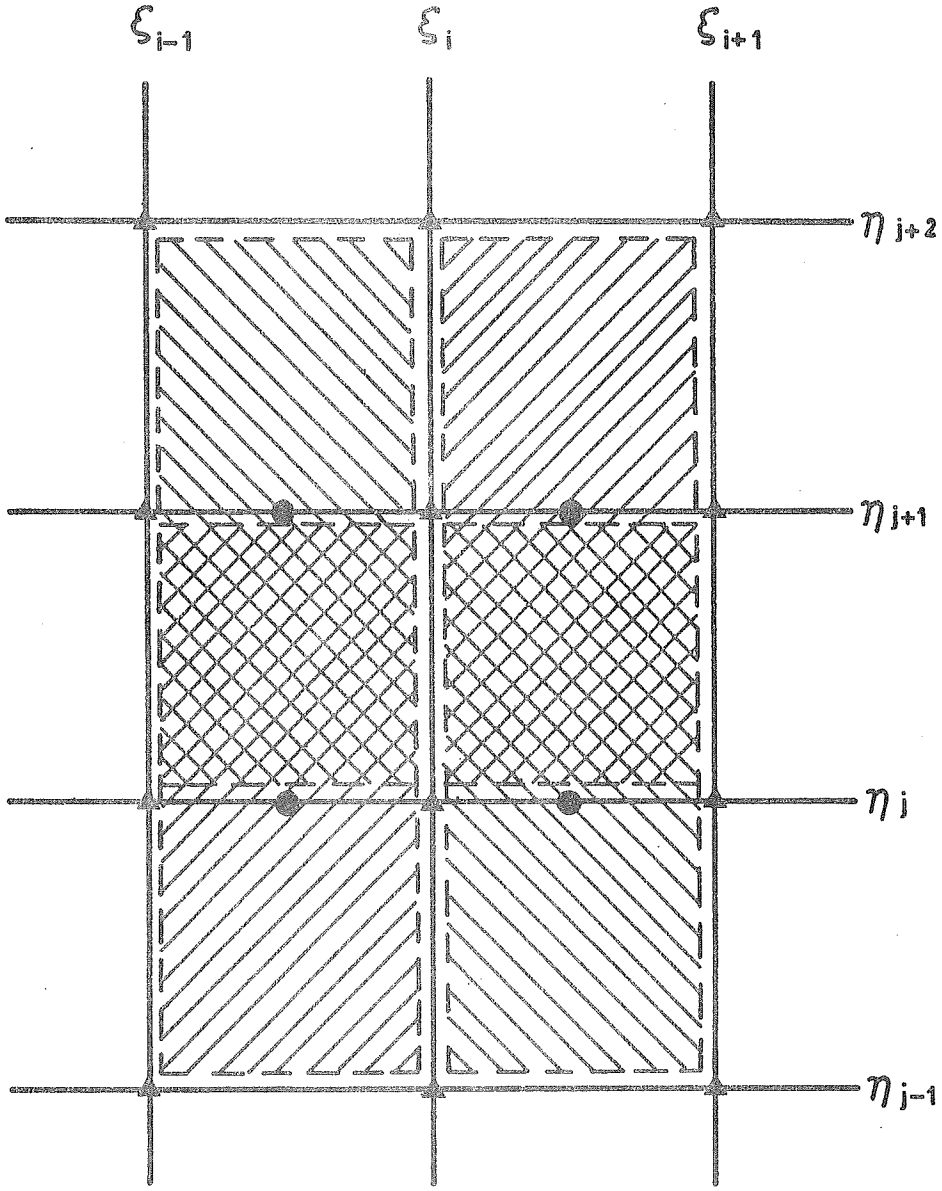

Fig.4 Overlapping Grid

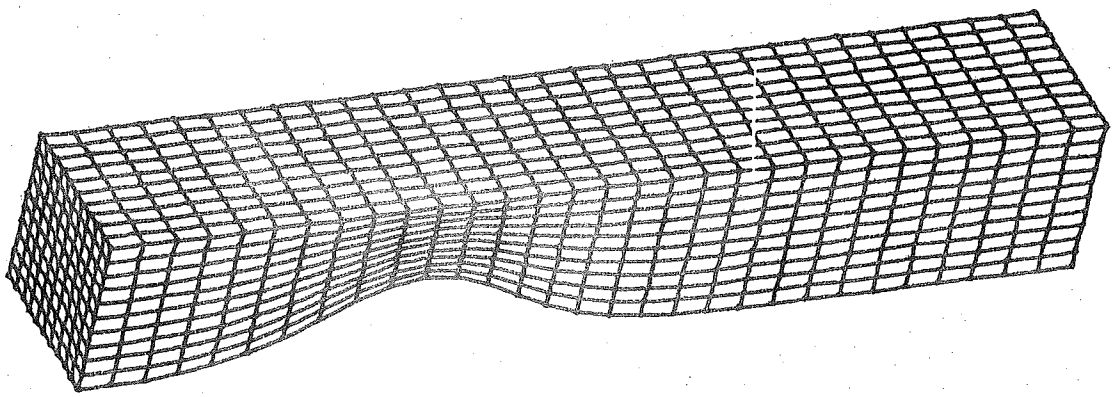

Fig.5a 3-D View of the Duct Mesh

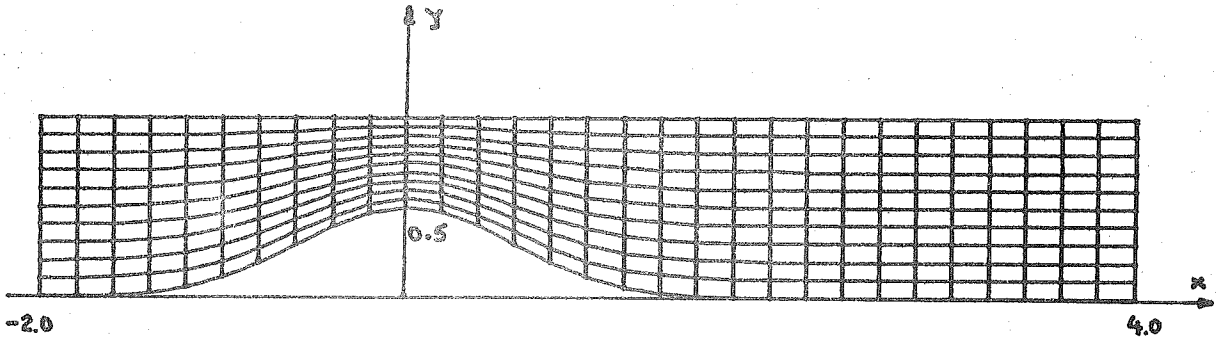

Fig.5b Dimensions in the plane ζ=const.

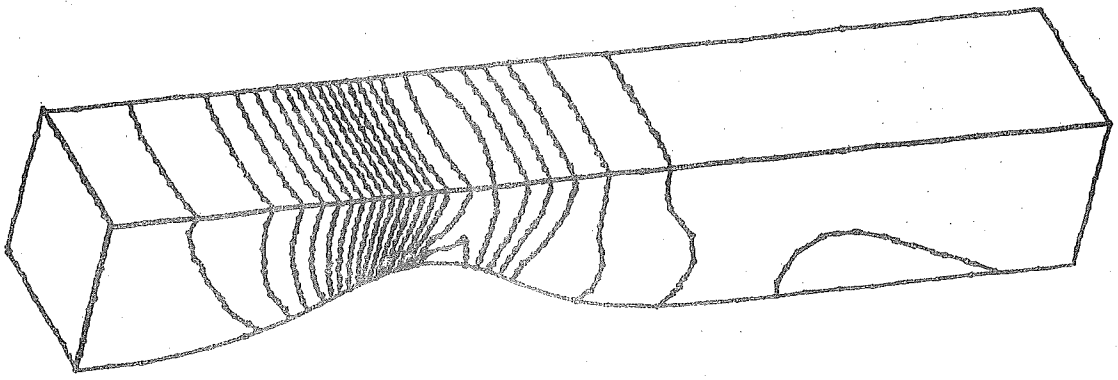

Fig.6a Static Pressure Isolines

i. In the plane z=0.1

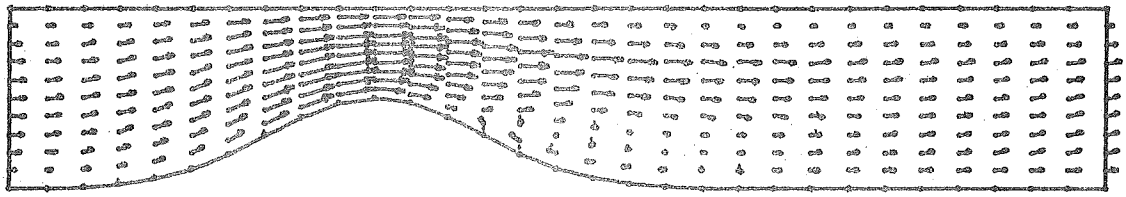

ii. In the plane z=0.5

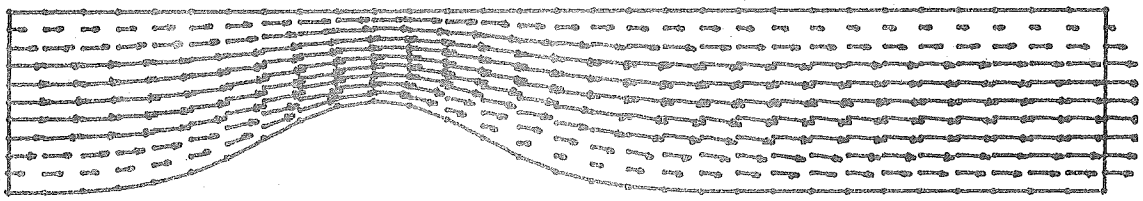

Fig.6b Velocity Field in planes ζ=const.,Re=80.

iii. η=0.9

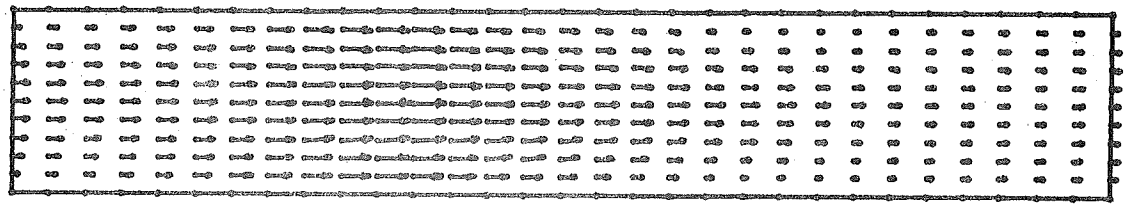

ii. η=0.5

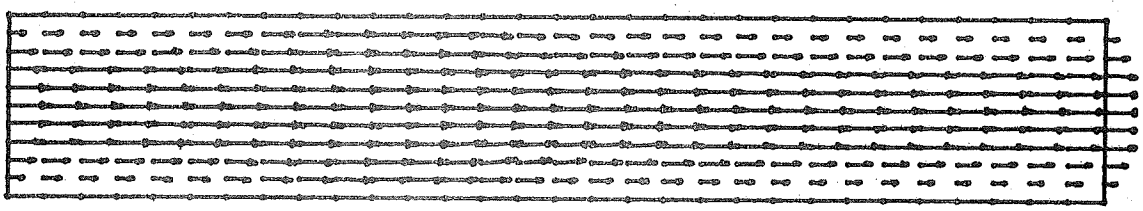

i. η=0.1

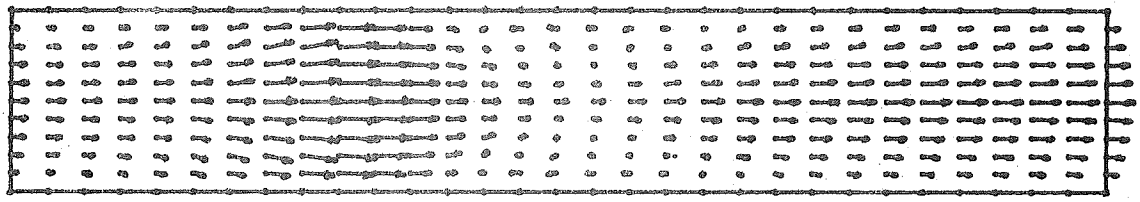

Fig.6c Velocity Field Projections of η=const. Surfaces

i. In Section x=-0.5

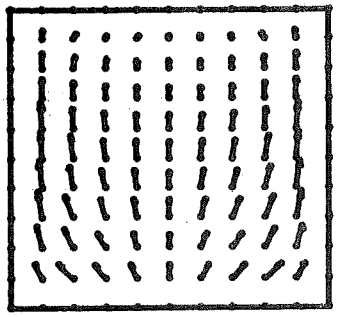

iv. In Section x=1.0

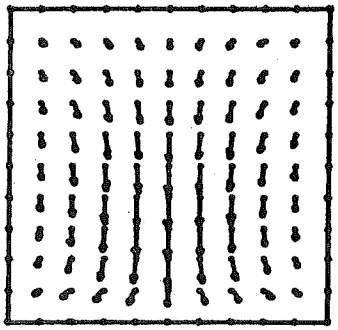

v. In Section x=1.5

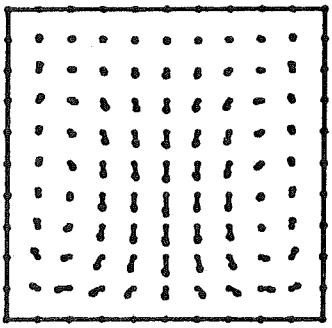

ii. In Section x=0.0

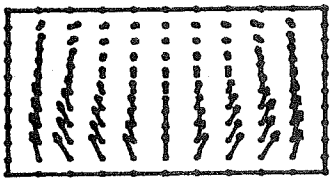

iii. In Section x=0.5

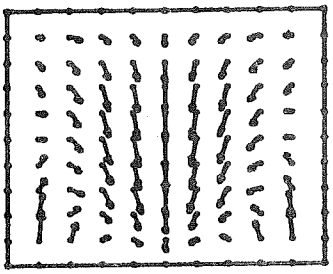

Fig.6d Velocity Development in ξ=const Surfaces

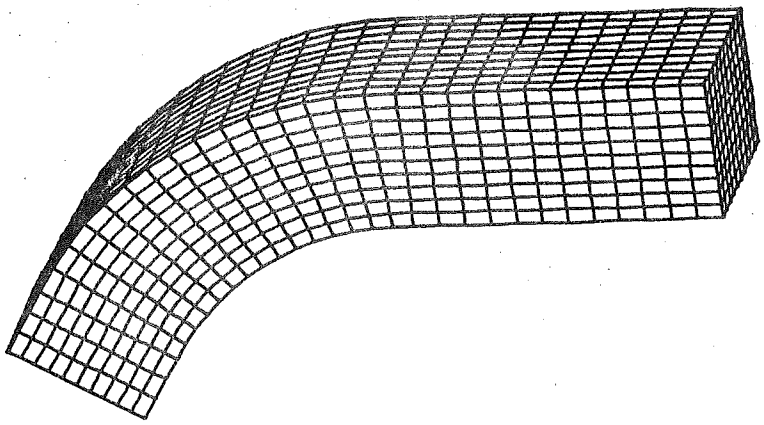

Fig.7a Circular Channel Grid

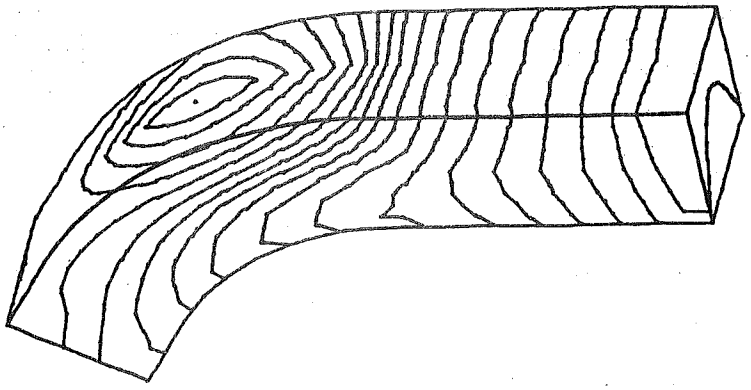

Fig.7b Static Pressure Distribution for Re=80.

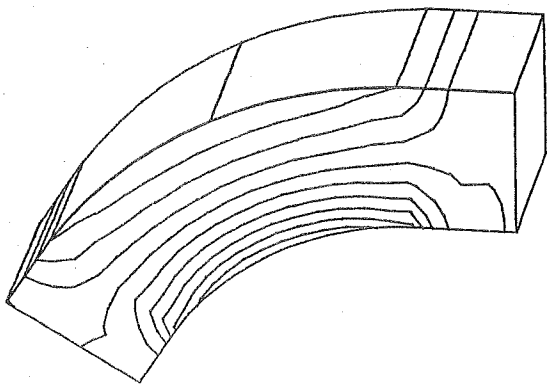

Fig.7c Potential Pressure Distribution(Ref. 14)

i. In Plane z=0.1

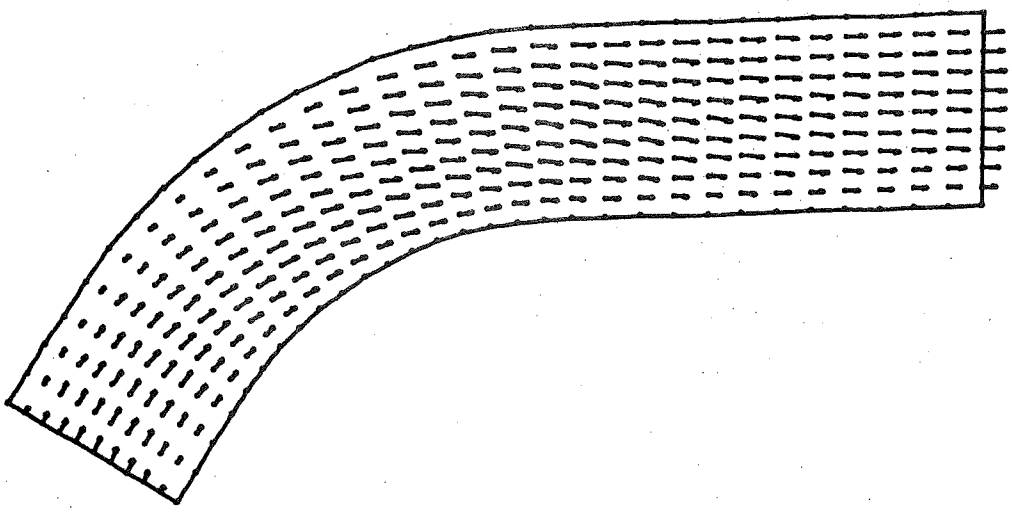

ii. In Plane z=0.3

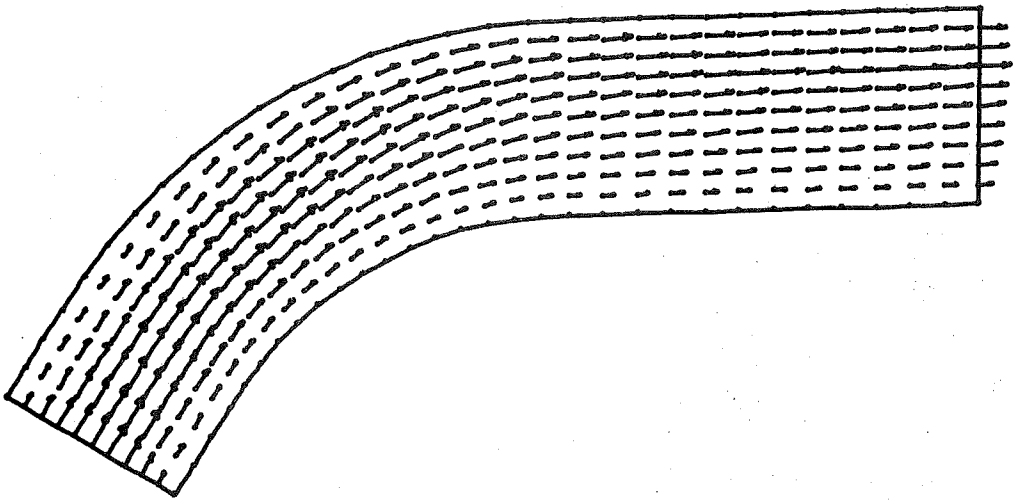

iii. In Plane z=0.5

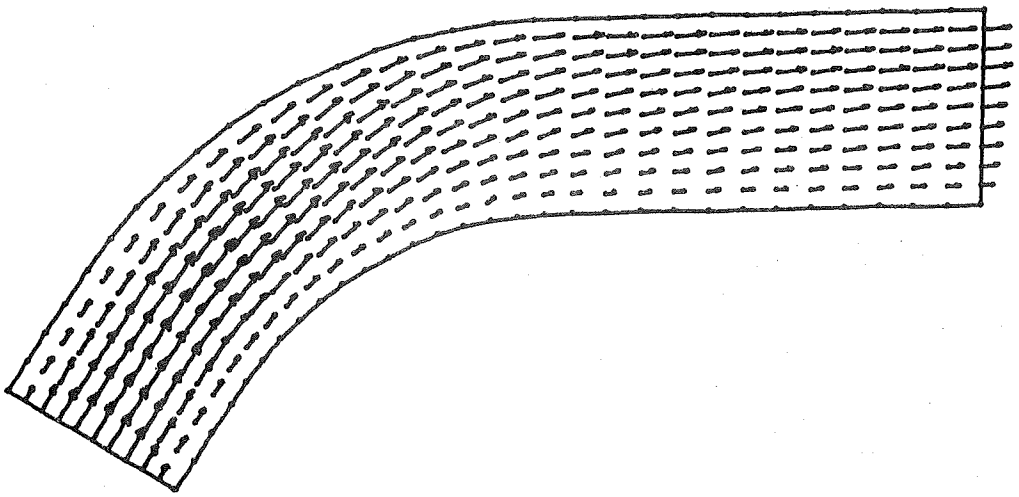

Fig.7d Velocity Field in planes ζ=const. for Re=80.

i. In Surface r=2.1

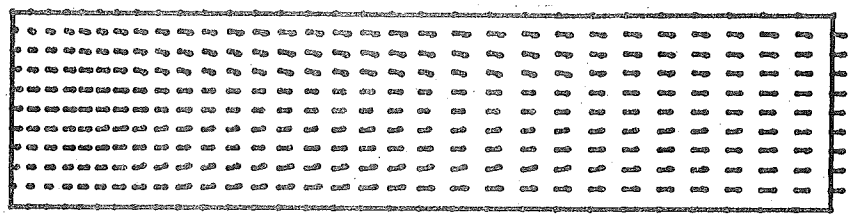

ii. In Surface r=2.5

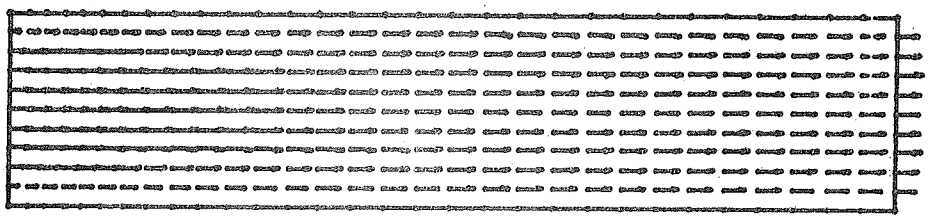

iii. In Surface r=2.9

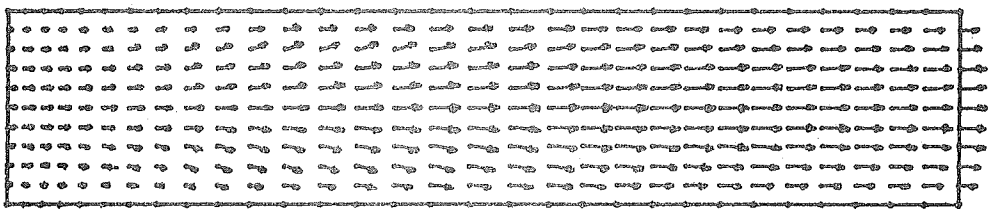

Fig.7e Velocity Field Projections of η=const. Surfaces, Re=80.

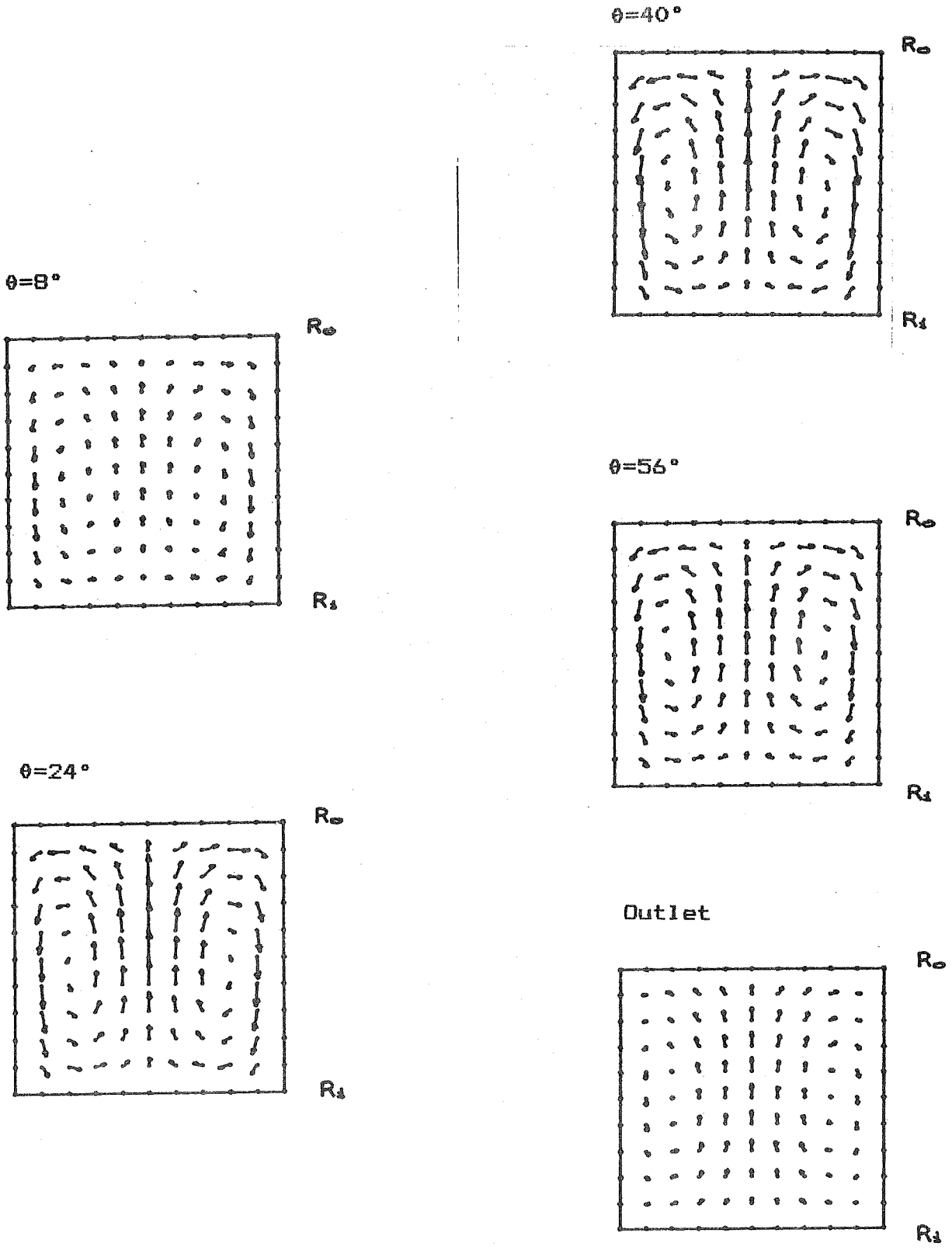

Fig.7f Developement of the Secondary Flow, Re=80.

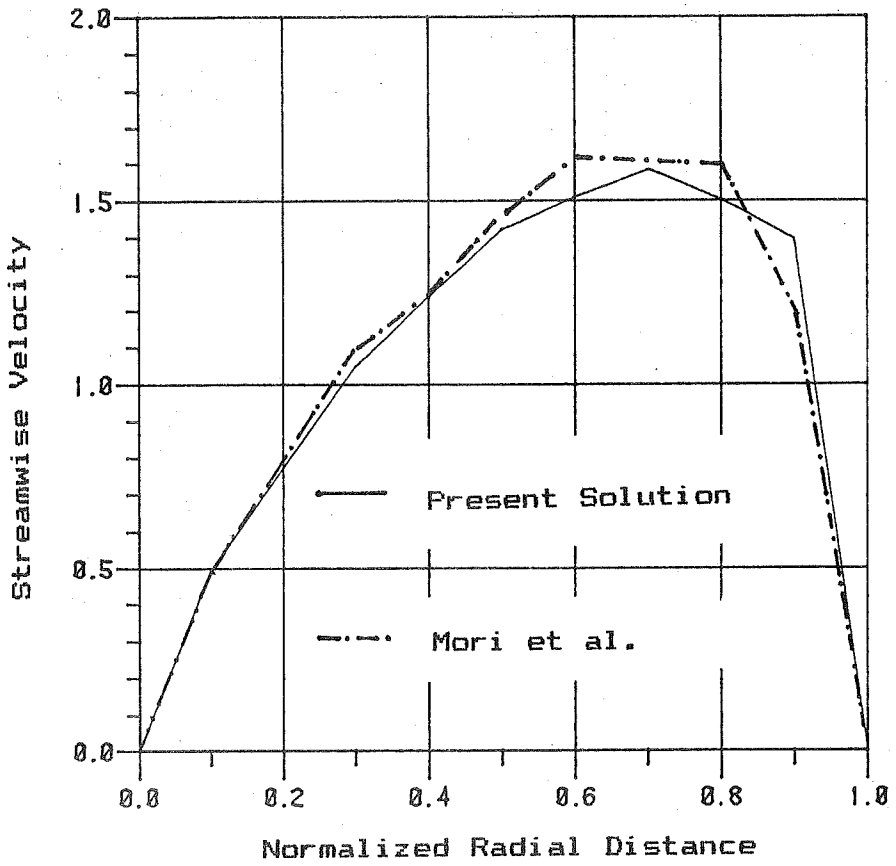

Fig.7g Fully Developed Streamwise Velocity Profile

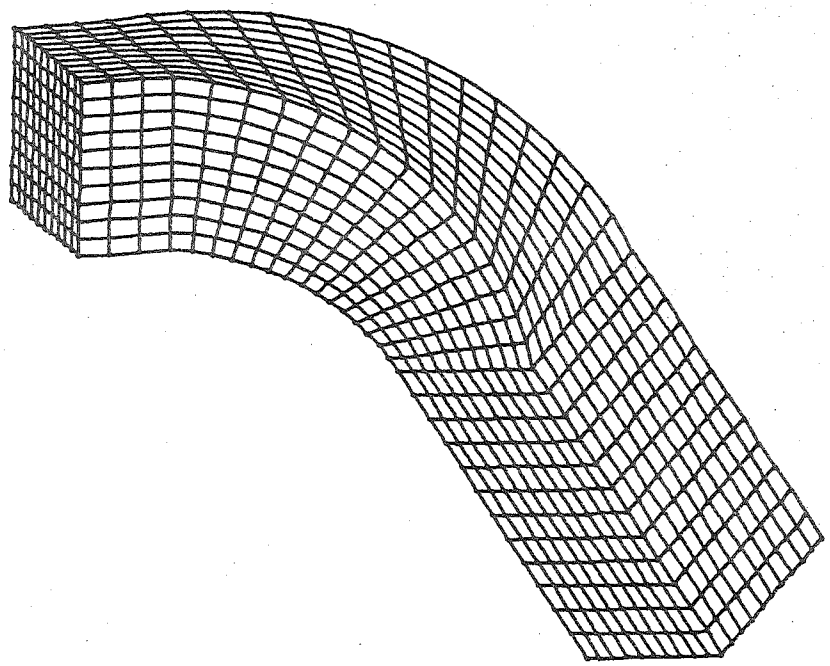

Fig.8a Twisted Elbow Representation

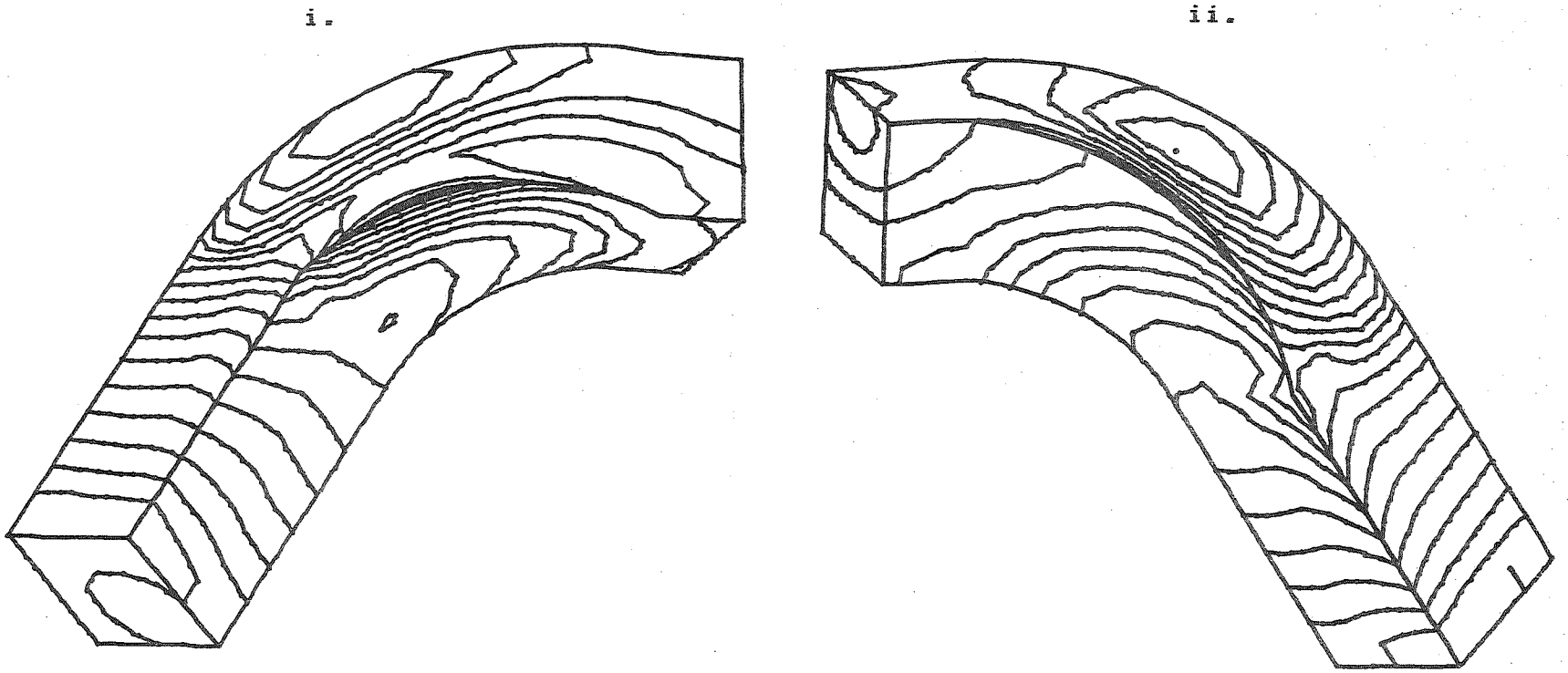

Fig.8b Isopressure Distribution on Outmost Surfaces

i. View form Back

ii. View from Front

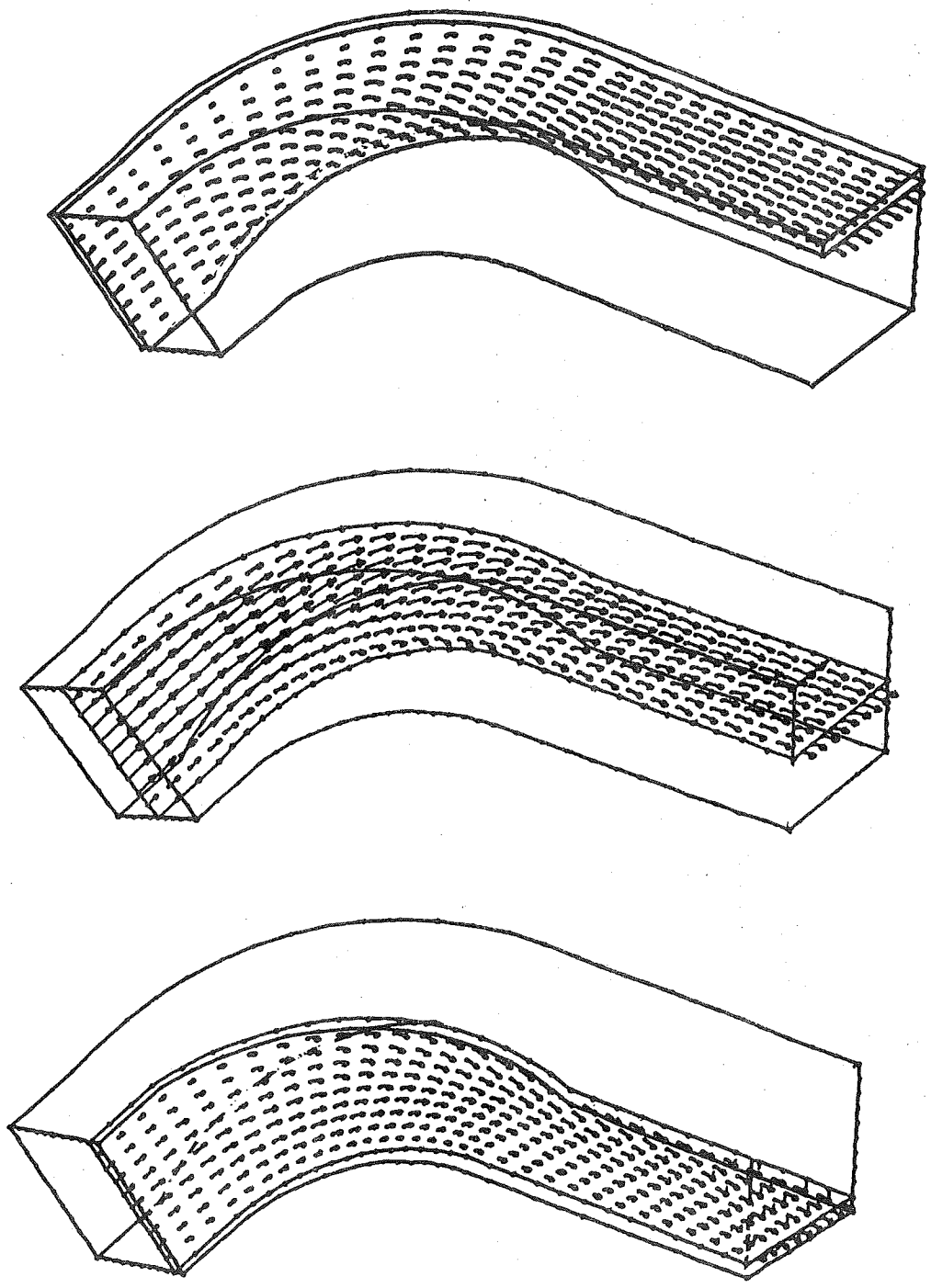

Fig.8c Velocity Distribution on ζ=const Surfaces.

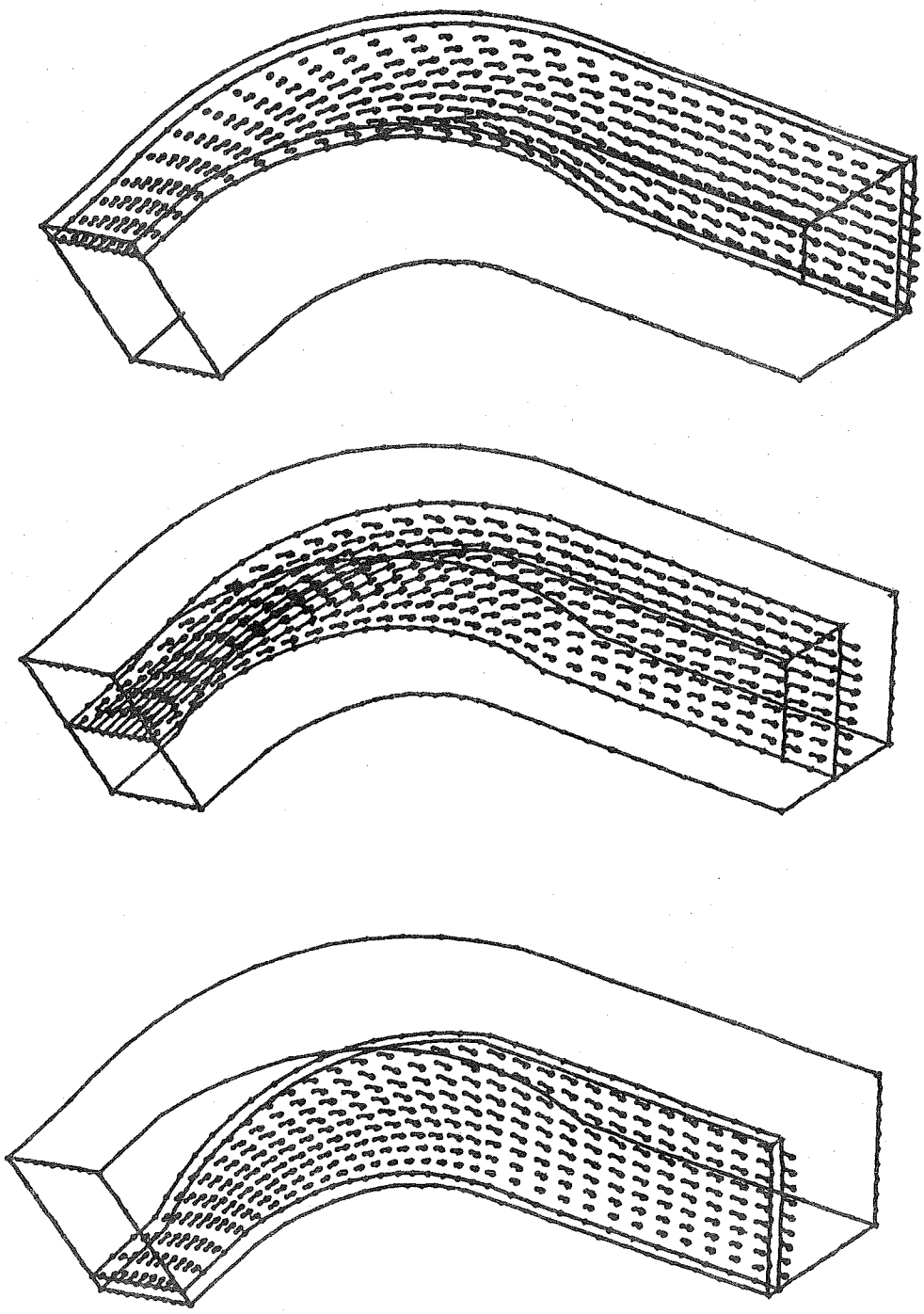

Fig.8d Velocity Distribution on η=const Surfaces.

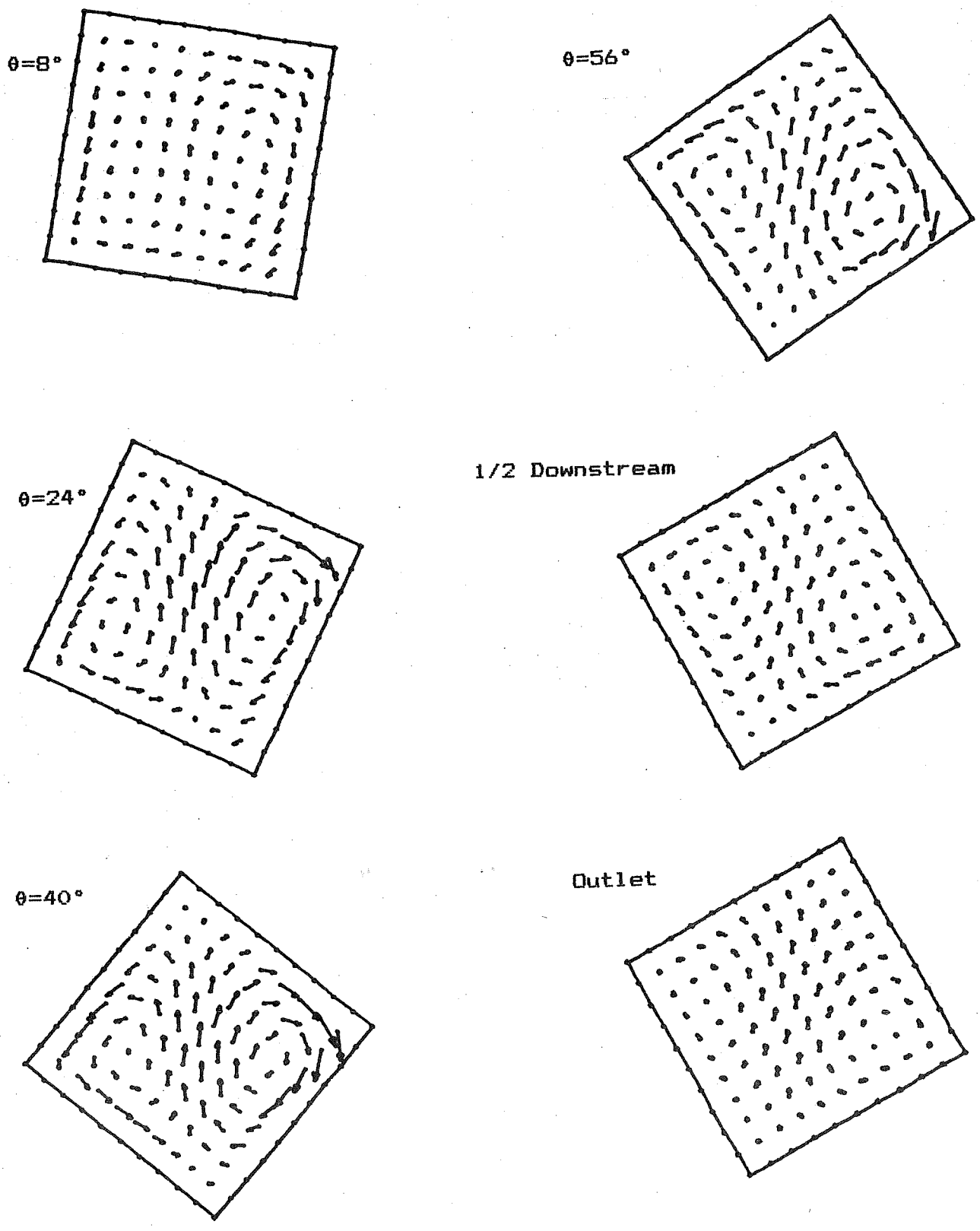

Fig.8e Development of the Secondary Flow, Re=80.